Chapter 4
Classification of Third Mobile Window Anomalies

Eugen Ionescu, Gerard J. Gianoli, and P. Ashley Wackym

Introduction

While superior semicircular canal dehiscence (SSCD) is relatively well-known in the medical community, there are many other sites of otic capsule dehiscence (OCD) which create a third mobile window resulting in third window syndrome (TWS). Over the past quarter century, there has been tremendous expansion of the depth of our knowledge and understanding of TWS; however, the identification of lesser-known sites of OCD remains an important diagnostic and therapeutic challenge. This is all the more so as in our experience TWS, including SSCD, remains under-diagnosed. Therefore, the development of a unitary anatomical-clinical and radiological classification would be an important step for a better understanding of these pathologies by neurotologists, otologists, neurologists, auditory-vestibular specialists, otolaryngologists, and neuroradiologists. Thus, the probability of being left without an etiological diagnosis in case of "mysterious" pseudo-conductive hearing loss, with or without obvious associated vestibular phenomena, should become lower. Furthermore, due to the progressive increase in new reported variants of OCD, the characterization of the anatomical structures involved, as well as the size and location of the TW, has become essential for a better understanding of the various mechanisms associated with this pathology. This allows us not only to

E. Ionescu (✉)
Service d'Audiologie et d'Otoneurologie, CHU Lyon, Institute de l'Audition, Paris, France
e-mail: eugen.ionescu@chu-lyon.fr

G. J. Gianoli
Ear and Balance Institute, Covington, LA, USA

P. A. Wackym
New Jersey, USA

G. J. Gianoli, P. Thomson (eds.), *Third Mobile Window Syndrome of the Inner Ear*, https://doi.org/10.1007/978-3-031-16586-3_4

systematize the different known variants but also to propose new, eventually less invasive or more pathophysiological therapeutic strategies. Based on the experience of the authors of this chapter, who have considered not only personal case studies but also other relevant publications on the subject, this chapter is the result of collaborative collegial work.

We are aware that there are several valuable articles in which an anatomical or radiological systematization of the lesions of the third window has already been proposed [1–6], however, in our opinion these authors did not propose a comprehensive unitary anatomical-clinical and radiological classification as presented here.

Please note that the authors have voluntarily excluded to review the tumoral, infectious, metabolic, or traumatic pathologies of the petrosal bone which can generate secondarily a TWS (e.g. glomus tumors, middle ear cholesteatoma, Paget's disease, perylimphatic fistula after fracture of the petrosal bone, etc.). It seems to us that it is easier to look for an area where the labyrinth is opened by a pathological process (thus generating a secondary TW), in the case of tumor or traumatic pathology of the petrosal bone, than to look for a "primary" OCD that is much less known or suspected by ENT specialists or radiologists.

Material and Methods

In the original paper proposing a unitary classification of third mobile window abnormalities [7], clinical and radiological data of 259 patients presenting a conductive hearing loss were retrospectively reviewed. Patients with degenerative processes or chronic infection of the petrosal bone, whether they underwent surgery or not, were excluded.

Due to the didactic purpose of this chapter, some other documented radiological data were used as well as audio-vestibular details from different relevant sources published previously.

Vestibular and Audiological Evaluation

Standard neurotological examination, including cranial nerve evaluation and otomicroscopy, was routinely performed in all patients. Pure tone audiometry (PTA; Madsen Astera-Otometrics), middle ear reflexes (Madsen Zodiac 901 tympanometer), videonystagmography including bone vibratory test (BVT) and valsalva maneuver (VNG, Ulmer SystemR; Synapsis SA), video head impulse test (VHIT, ICS Impulse R; GN Otometrics), cervical vestibular evoked potentials (cVEMPs), and ocular vestibular evoked potentials (oVEMPS) (Bio-Logic RNav-Pro system) in air conduction with 750 Hz stimuli were systematically performed in all patients.

Radiological Assessment

(a) Petrous bone high-resolution CT (GE GSI Revolution, GE Healthcare, USA) was performed in all patients. Slices were acquired helically in the axial plane at a nominal thickness of 0.625 mm with a 50% overlap of 0.312 mm, as recommended [8–10]. Images were obtained in ultra-high resolution at 140 kV and 200 mAs/section. The primary images were reworked in the axial and coronal planes of the lateral CSC at a 60 mm field of view with a 512 matrix for an isometric voxel. Pöschl plane (i.e., superior SCC plane) using Advantage Workstation (AW) Server visualization software (GE Healthcare, USA) was also employed.

(b) Additionally, 3 Tesla MRI (3T MRI; GE Healthcare, Philips Ingenia, Philips healthcare) of the petrous bone and inner ear structures was also performed if associated pathologies were suspected, or when vestibular and/or vascular structures appeared to be involved at the TW's interface. 3D T1-weighted contrast enhanced sequences allowed for confirmation of the vascular nature of the involved structure, and the HR 3D T2 labyrinth sequence DRIVE (DRIVEN Equilibrium pulse, TE 157, TR 1000, slice thickness 0.4, Turbo factor 40, Matrix 500 × 500, voxel size: 0.4 × 0.4 isotropic) highlighted, when necessary, the morphology and permeability of the membranous labyrinth. Fused images between CT slices in Pöschl plane and 3D T1 weighted contrast enhanced sequence obtained with post-processing software (AW Server, GE Healthcare) were performed to assess the TW interface.

Results

Following this analysis, a classification of OCD was proposed based on the anatomic structures and radiological features involved at the TW partition (Table 4.1). A list of the most frequent symptoms from the initial series was included.

Table 4.1 Third mobile window abnormalities (TMWA): classification and clinical elements

	Interface	Type	Number of patients	Clinical features	cVEMP thresholds
Extralabyrinthine TMWA (OCD)	OC-Meningeal	I	48	Vertigo (42%) Auditory symptoms (35%)	Decreased (20%)
	OC-Vascular	II	28	Vertigo (64%) Auditory symptoms (64%)	Decreased (14%)
	OC-Petrosal	III	17	Vertigo (47%) Auditory symptoms (52%)	Decreased (21%)
Intralabyrinthine TMWA -like	Vestibular aqueduct - Posterior SC		4	Vertigo (50%) Auditory symptoms (25%)	Decreased (0%)
Multiple OCD	Multiple locations (on the same ear)	/	11	Vertigo (80%) Auditory symptoms (100%)	Decreased (40%)

SC, Semicircular Canal; OCD, Otic Capsule Dehiscence

Type I: OCD-Meningeal

This type (Fig. 4.1) includes two main subsets that were historically the first cases of dehiscence described in the literature:

Subtype Ia

This type refers to the SSCD described by Minor, in which the SSC is typically in contact with the dura of the middle cerebral fossa (Fig. 4.1a, b).

Subtype Ib

This type of dehiscence involves the posterior SC (PSC), which can be in contact with, or very close to, the dura of the posterior fossa (Fig. 4.1c, d). As in the Type Ia, Type Ib may be present bilaterally. The pathophysiological mechanism for this type, including its two sub-variants, was largely described previously.

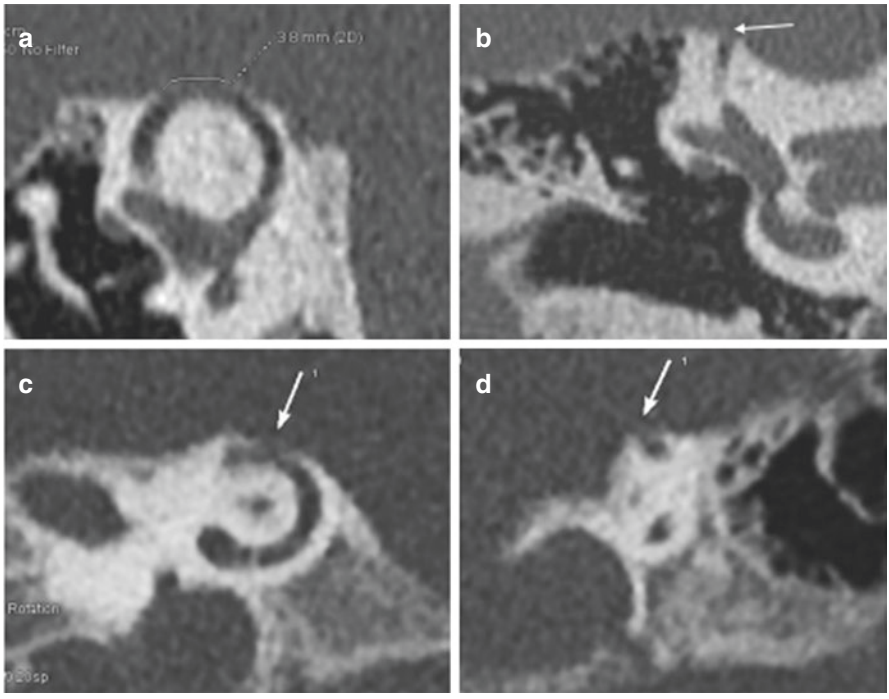

Fig. 4.1 Type I otic capsule dehiscence (OCD) (OC-meningeal interface). (**a**, **b**) Superior semicircular canal dehiscence (SSCD); (**c**, **d**) Posterior semicircular canal dehiscence (PSCD)

In air conduction (sounds frequencies ranging from 500 to 2000 Hz) the perilymph-driven hydraulic acoustic pressure, which normally reaches the round window, dissipates toward the dehiscence where a drop in impedance occurs, resulting in increased audiometric thresholds [11–13]. According to Iversen and Rabbit [11], the resultant biomechanical phenomena in the membranous SC can lead to an opposite neural vestibular response at the level of the cupula depending on the frequency of the stimulus, with a decrease and increase of the afferent firing rate for low and high frequencies, respectively. In bone conduction, the decrease in impedance favors the gradient between the vestibular and tympanic ramps and leads to a lowering of the thresholds. Application of a loud sound or pressure in the external auditory canal (EAC) potentially gives rise to an excitatory ampullofugal flow in the SSC. In addition, performing a Valsalva maneuver, by pinching the nostrils, classically results in ampullofugal movement [14]. Ampullopetal (inhibitory) flow is then attained by applying negative pressure in the EAC, or from a closed glottis Valsalva maneuver (increased intracranial pressure) (Fig. 4.2a, b).

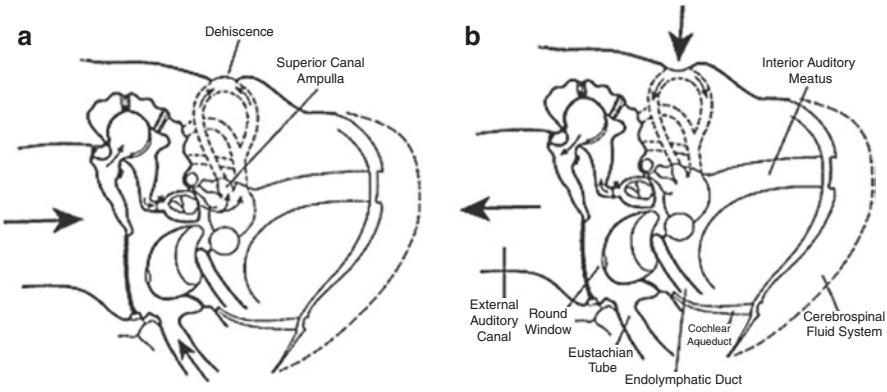

Fig. 4.2 Type I OCD's mechanism: (**a**) Sound, positive pressure in the external canal, and Valsalva maneuver against pinched nostrils evoke pressure changes that result in expansion of the membranous canal with corresponding outward movement in the area of dehiscence. Such pressure within the membranous canal causes ampullofugal deflection of the superior canal cupula that results in excitation of vestibular-nerve afferents innervating the ampulla. (**b**) Valsalva maneuver against a closed glottis, bilateral jugular venous compression, and negative pressure in the external canal result in inward movement in the area of dehiscence of the superior canal. Such pressure leads to ampullopetal deflection of the cupula and inhibition of the superior canal. *Reproduction with permission from Lloyd Minor [14]

Type II: OCD-Vascular

This type (Fig. 4.3) of dehiscence correlates with a contact between the membranous vestibular or cochlear labyrinth and a vascular venous or, less frequently, arterial structure. It includes subtypes IIa, IIb, and IIc.

Subtype IIa

This type involves vasculo-vestibular contact between the membranous SSC and the superior petrous sinus (SPS) (Fig. 4.3a–c). Interestingly, in our reported series [7] there was no evidence of a "true" Tullio phenomenon, including nystagmus elicited by loud sound stimulation, in this group of patients. Moreover, the Valsalva maneuver against the closed glottis did not cause true vertigo except for slight "dizziness" in a few cases. Instead, during this maneuver, an increase in the intensity of their pulsatile tinnitus was constantly reported. This subtype can also integrate SSCD-subarcuate artery dehiscence and SSCD-superior petrosal vein dehiscence variants [15].

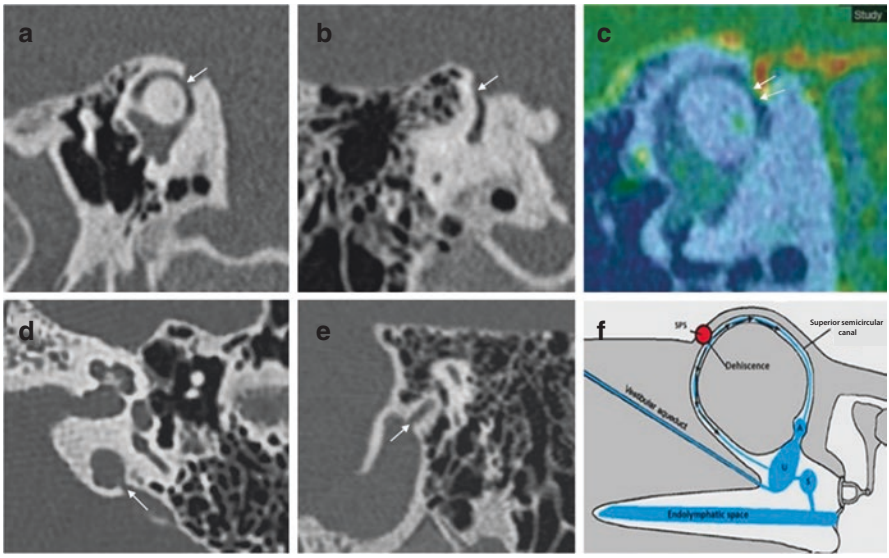

Fig. 4.3 Type II extralabyrinthine OCD (OC-vascular interface). HRCT in the plane of the superior (Poschl) denuded SSC (white arrows) (**a**, **b**), 3T MRI labyrinthine, fused image between 3DT1-weighted contrast enhanced sequence and 3DT2 DRIVE sequence: Mass effect exerted by the Superior Petrosal Sinus (SPS) against the membranous SSC (yellow arrows) (**c**). High-resolution CT (HRCT) in axial plane (**d**), coronal plane (**e**): contact between the denuded VA and the IJV (white arrows). Proposed schematization of the mechanism of vestibulo-vascular TW. Pulsations of the interested vascular wall in intimate contact with the otic capsule membrane would cause non-physiological stimulation of the cochlea and/or the nearest vestibular sensory organs (**f**): Membranous SSC in contact with the SPS

Subtype IIb

This concerns OCD involving the internal jugular vein (IJV) and various vestibular structures. A dehiscence involving the vestibular aqueduct (VA) in contact with the IJV (Fig. 4.3d, e) was the second most prevalent variant series as it was diagnosed in 19 out of 97 patients [7]. This presentation may be bilateral as well. Variant between IJV and PSC was identified in fewer patients. A dehiscence involving the IJV and the cochlear aqueduct (CA) was found to be rarer since in the above-mentioned study only three ears (left-sided) in two patients, age varying from 12 to 53 (1M, 1F) was diagnosed. In subtype IIb OCD, vertigo and/or pulsatile tinnitus induced by exertion were constantly reported. Positional vertigo was also a commonly reported symptom with no evidence for true benign positional paroxysmal vertigo (BPPV) episodes.

Subtype IIc

In this subtype the OCD is localized between the membranous cochlea and the intrapetrous carotid artery [16]. Pulsatile tinnitus exerted by physical exercise synchronous with the peripheral pulse is specific for this variant. The pathomechanism of the inner ear ends structures' stimulation does not seem obvious. However, it can be hypothesized that, compared to type I dehiscences, in type II dehiscences non-physiological audio-vestibular stimulation can be produced by the vascular structure pulsations [17] (Fig. 4.3f). Thus, the vibrations generated by the vascular wall, in contact with the perilymphatic space, will generate symptoms of intensity (pulsating tinnitus and/or dizziness) depending on the location, surface, and importance of any mass effect exerted by the vessel on the labyrinthine structure at the TW level [5].

Type III: OCD-Petrosal Bone

This type encompasses all OCD variants (with to date only three reported subtypes) in which the membranous labyrinth is in direct contact with pneumatic elements of the temporal bone. The difference between this OCD type and a perilymphatic fistula (PLF), which may generate similar symptoms, consists in the integrity of the labyrinthine membrane which is disrupted allowing endolymphatic fluid leak in the case of PLF.

Subtype IIIa

It involves a communication between the cochlea and the facial nerve canal - or cochlear-facial dehiscence (CFD) (Fig. 4.4a, b). In these patients, autophony and slight conductive hearing loss were predominant. Dizziness related to loud sounds

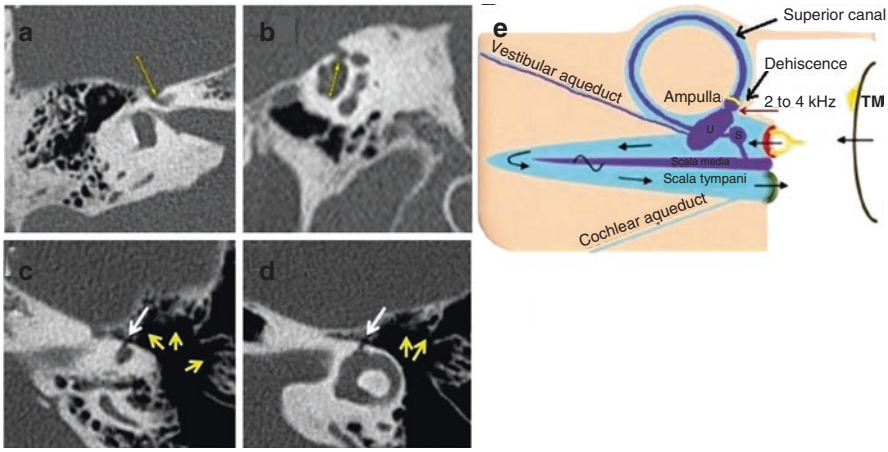

Fig. 4.4 Type III extralabyrinthine OCD (OC-petrosal interface). Right ear cochleo-facial dehiscence (CFD): the second turn of the cochlea dehiscent on the facial nerve canal in its geniculate zone (or the first segment of the facial nerve canal) on axial section or coronal oblique section (**a**, **b**). Ampullary dehiscence (white arrow) localized on the LSC (**c**, **d**). Note the hyper pneumatization of the mastoid and attical regions (yellow arrows). Proposed mechanism's schema in this variant of ampullary dehiscence, which relies on a principle similar to a Helmholtz resonator. T M, tympanic membrane (**e**). *Modified with permission from Rosowski [1] and from Ho [3]

or physical exercise was frequently described. Affected attention, difficulty judging distances, and migraines or chronic equivalents have also been reported frequently [16, 18].

Subtype IIIb

It includes a dehiscent surface between the membranous labyrinth and some hyperpneumatized mastoid air cells freely communicating with the tympanic cavity. This variant was for the first time reported in one 60-year-old male patient [19] in which a strong Tullio phenomenon, associated with a typical down-beating nystagmus indicating a stimulation of the left SSC, was highlighted by a left auditory stimulation at 120 dB between 2 and 4 kHz, although there was no conductive hearing loss. Hyperpneumatization of the petrous bone appears to play an important role in the pathomechanism of this rare OCD. HRCT showed a significant number of large mastoid air cells communicating with the tympanic cavity (Fig. 4.4c, d) and they appear to be in intimate contact with the membranous SSC and the lateral SC (LSC), respectively, via an ampullary located dehiscence of maximum 1.5 mm width. The disposition of these mastoid air cells would act as an acoustic amplifier like the physical principle of a Helmholtz resonator (Fig. 4.4e). Thus, the sound vibrations

transmitted via the tympanic cavity and amplified at the mastoid cell/ampullary vestibular membrane interface will directly stimulate the cupula of the concerned SSC. As this hypothesis does not imply a significant acoustic energetic shunt toward the posterior labyrinth, it could therefore explain the absence of conductive hearing loss. Although the lateral SC ampulla also appeared dehiscent (Fig. 4.4c, d), most likely the air cells adjacent to this structure did not communicate with the tympanic cavity, and the above SSC therefore remained asymptomatic.

Subtype IIIc

It includes cochlear (or labyrinthine) dehiscence over the internal auditory canal (IAC), a "near" dehiscence of this subtype is indicated in Fig. 4.6a.

Intralabyrinthine Third Mobile Window-Like Variants

This subgroup corresponds to an abnormal contact between two membranous parts of the same labyrinth being constantly associated with limited inner ear anomalies. For example, dehiscence involving a dilated endolymphatic sac (Fig. 4.5a, b) or a similar presentation involving an EVA in contact with the ampulla of the PSC. Some anatomical variants or other forms of intralabyrinthine TMWA sharing similar

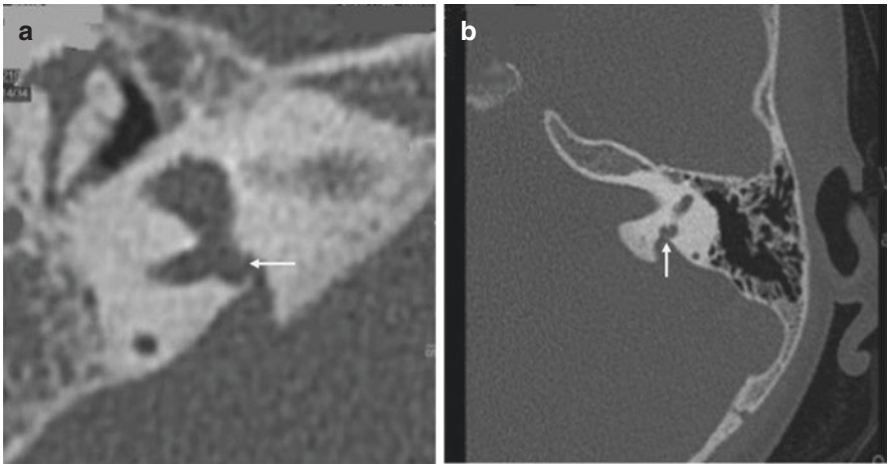

Fig. 4.5 Intralabyrinthine TMWA-like. (**a**), Vestibulo-vestibular dehiscence: between the vestibular aqueduct (VA) widened to 3 mm (white arrow) and the right posterior SC (white arrow) - right ear; a similar variant on the left ear between an enlarged VA and the SSC at the level of the common crus (**b**)

symptoms could be included in this subtype. Pathophysiological mechanisms, including changes in endolymphatic flow caused by the presence of dilatation of the vestibular organs or the presence of intralabyrinthine obstacles (fibrosis, tumors), primary or secondary endolymphatic hydrops, may be included. Matsuda et al. [20] recently reported the case of a congenital dehiscence of the stapes footplate in a patient presenting a sudden right-sided hearing loss and severe vertigo that occurred immediately after nose-blowing. These last-mentioned variants, associated with challenging clinical pictures, allow us to insist and emphasize the importance of careful and collaborative study of audio-vestibular exams and imagery for the sake of finding the diagnosis in certain "unexplained" symptoms. Some authors considered an isolated EVA or enlarged cochlear aqueduct as a distinct TW, since the perilymphatic normal flow transporting the acoustic energy to the cochlear end receptors is disrupted [1]. We agree with this vision although these pathological conditions are not generated by a "true" OCD, but the intimate mechanism seems quite similar to that of a third mobile window. Therefore, we could include these cases in the class "intralabyrinthine TMW" or having a TMW-like mechanism, in addition to intracochlear schwannomas (ICS) that could induce modifications of the endolymphatic flow. Indeed, in a cohort of 19 patients with ICS, Fröhlich et al. measured the cVEMPS thresholds [21]. On the affected side, the threshold was unexpectedly lowered in 21% of patients mimicking the presence of a TMW. The authors suggested that individualizing the management of these patients with a detailed functional evaluation of the labyrinth is paramount for proposing treatment options and predicting outcomes. As a physiological explanation, the authors mentioned changes in endolymphatic flow secondary to tumor obstruction in a similar manner to endolymphatic hydrops. It has already been shown that some cases of endolymphatic hydrops can mimic the TW syndrome with a similar clinical presentation [22–25]. Besides, primary overpressure in the endolymphatic or perilymphatic spaces could explain a limited conductive hearing loss as previously reported [26–28]. It is worth adding here that the notion of "inner ear conductive hearing loss," considered lately as specific to TW lesions, was already used by Muchnik et al. to describe the air bone gap (ABG) observed in some patients with Ménière's disease [26]. Other TMWA-like pathologies may include perilymphatic fistula (PLF). Although it may appear anatomically like type III extralabyrinthine OCD, clinical evidence indicates the involvement of other endolymphatic flows generating nystagmus with different characteristics [8]. Some authors have reconciled PLF with OCD because of similar pathophysiological elements [9, 16]. The explanation for some clinical differences may lie in the fact that in PLF, the vestibular membrane is compromised at this level while in type III, it remains intact. Hence, PLFs have not been considered in our classification as "true TW" because they involve an opening of the membranous labyrinth that allows the leakage of perilymph and/or endolymph with the obvious direct negative impact on the vestibulocochlear micromechanics.

Multiple OCD Localizations

There is more and more evidence that multiple OCD localizations (Fig. 4.6a–c) are not rare. See Table 4.2 for the most common symptoms found in multiple localization series as well as the most common associations on the same ear; the most important audiological and vestibular data are also displayed. Besides an accurate and complete diagnosis, the main challenge in multiple OCDs in the same ear is to select an appropriate therapeutic strategy for patients with disabling symptoms. It also involves establishing the order in which these multiples dehiscences should be treated. At the time of publication, according to our knowledge there are no available data or consensus in the literature to council practitioners about the approach of multiple OCDs.

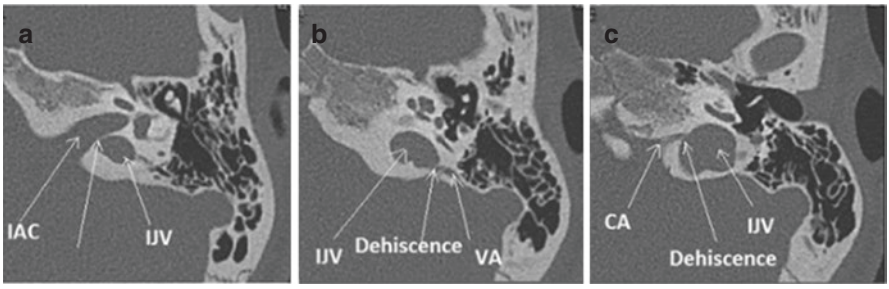

Fig. 4.6 Multiple localization OCD: high riding left IJV at the origin of two type II of OCD. Near dehiscent jugular bulb in the IAC (White arrow), a thin bone lamina is remaining (**a**); Dehiscence between IJV interface and VA (**b**); Dehiscence between IJV interface and CA (**c**). *IJV* internal jugular vein, *IAC* internal auditory canal, *VA* vestibular aqueduct, *CA* cochlear aqueduct

Table 4.2 Clinical characteristics of patients with multiple localization OCD (all OCD were ipsilateral)

Age	Ear	1st OCD dehiscence	2nd OCD dehiscence	Symptoms	Audiometry findings	oVEMPs	oVEMPs
16	RE	PSC-IJV	CFD	Tinnitus with head movement Noise-induced vertigo	Mild Hearing loss ABG = 5 (RE)	Bilateral threshold (x2)	Higher amplitude (RE)
37	RE	SSC-SPS	CFD	Pulsatile tinnitus (RE)	Normal	Higher amplitude (LE)	Absent
48	LE	SSC-Meningeal	CFD	Noise-induced autophonia pulsatile tinnitus (LE)	Bilateral low-frequency hearing loss ABG = 5 bilateral	Higher amplitude (LE) Threshold 60 dB (LE)	Higher amplitude (LE) Threshold 60 dB (LE)
73	RE	SSC-Meningeal	CFD	Decreased hearing Tinnitus Autophonia Cough-induced vertigo	ABG = 30 dB (RE)	Higher amplitude (RE) Threshold 60 dB (RE)	Higher amplitude (RE) Absent (LE)
68	LE	SSC-Meningeal	Cochlea-Carotid	Decreased hearing	Mixed HL ABG = 50 dB (RE) SNHL (LE)	NA	NA
59	LE	IJN-Vestibular aqueduct	CFD	Tinnitus (tapping) (LE) Instability and vertigo	ABG = 10 dB (RE) 20 dB (LE)	Normal	NA
67	LE	IJV-Vestibular aqueduct	IJV-IAC	Pulsatile tinnitus (RE)	Normal	Normal (RE) Absent (LE)	NA
46	LE	SSC-Meningeal	CFD	Bilateral HL Tinnitus (RE) Effort-induced vertigo	ABG = 20 dB (RE) Bilateral SNHL	Absent (RE) Decreased threshold 60 dB (LE)	Absent (RE) Decreased threshold 70 dB (LE)
72	RE	SSC-Meningeal	IJV-Vestibular aqueduct	Autophonia Pulsatile tinnitus Effort-induced vertigo	Bilateral SNHL	Threshold 50 dB (RE) Normal (LE)	NA
13	LE	IJV-Vestibular aqueduct	IJV-Cochlear aqueduct	Effort-induced vertigo	Normal	Normal	NA

CT-OCD or Not Identified OCD (NIOCD)

As introduced by Shuknecht [10] at the early age of deafness surgery, Wackym et al. [29, 30] reported patients with a group of symptoms suggestive of OCD, even if the imaging was negative. In these patients, the presence of a possible OCD may also be indicated by the presence of cervical or ocular VEMPs below the normal threshold. According to these newly described (or future) variants of OCD, performing temporal bone HRCT with infra-millimetric slice thickness as recommended can be of great benefit in the diagnostic process in such symptomatic patients, and in search of all possible types of OCD [14, 31].

A particular subtype that can be included here is the "Near Dehiscence Syndrome" (NDS). As described by several authors [32, 33] the third mobile window syndrome may be present, even partially, in the case of significant bone thinning of confirmed SSC either by HRCT or when no frank dehiscence was found intraoperatively. Although NDS has not yet been reported at other sites, physiologically there is no reason to think that this could not be present elsewhere.

Perspectives

Superior semicircular dehiscence has been the subject of numerous articles codifying its surgical management [34]. Concomitantly, with a better understanding of the OCD pathophysiology, new therapeutic procedures have emerged to diminish operative risks. Creighton et al. described the case of a patient with a SSCD who benefited from an endoscopic "underwater" procedure in a balanced salt solution [35]. This attempt was aimed at limiting the risk of PLF by injecting fluid into the mastoid, as a counter pressure method during the plugging procedure. From our perspective, the major principle to be considered in the future for the treatment of TW lesions would be to find the most appropriate methods that aim at reducing the abnormal transmission of sound vibrations through the abnormal window to the vestibular and/or to cochlear end organs, without excluding any highly functional labyrinthine segment. A step forward would possibly be the manufacturing of a physical or a numerical semicircular model, which would allow for a better pathophysiological approach and management of these challenging pathologies. With the actual constraints and ethical considerations in clinical medical research, this method could be promising. Such a model could allow researchers to obtain a "near real" simulation of volumetric and pressure changes in the endolymphatic system generated by the various surgical procedures proposed in this pathology. This could avoid certain negative postoperative outcomes seen in a number of patients and, most likely, new surgical techniques or improvement of existing ones. Furthermore, it may be the ideal way to manage and possibly resolve certain complex pathophysiological and treatment dilemmas, such as therapeutic choice in multiple OCD locations.

Conclusions

Based on anatomo-radiologic data of the inner ear structures involved, a classification of TMWA is proposed in this chapter (Fig. 4.7a, b). Although some systematizations of this pathology have been proposed previously, we believe that this new classification that considers not only the anatomical structures involved in the TW interface, but also their precise topographic localization, would lead to a better further understanding of the underlying pathophysiological mechanisms of this pathology. Moreover, the present classification could allow ENT specialists, researchers,

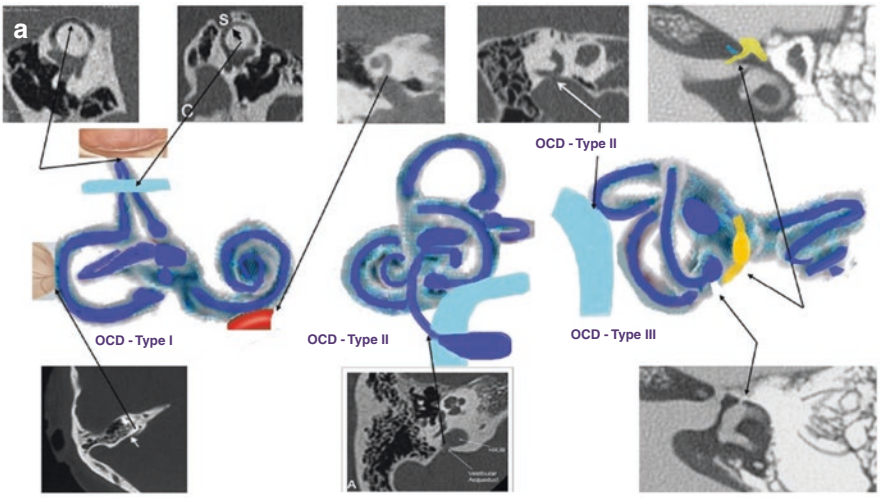

Comprehensive scheme including all OCD variants (three type OCD)

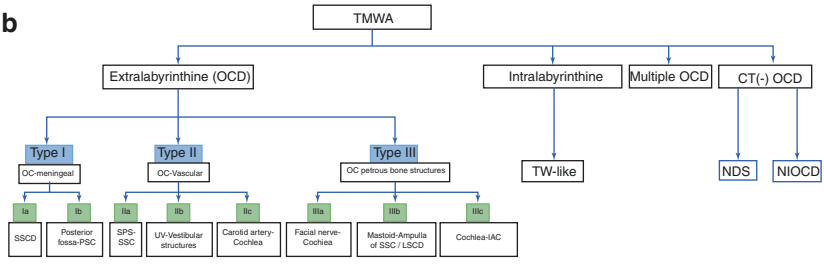

Comprehensive scheme of TMWA including all OCD variants

Fig. 4.7 (**a**) 3 type extra labyrinthine OCD classification in images—correspondence between imagery and anatomic variants. (**b**) Comprehensive algorithm of third mobile window (TMWA) anomalies classification. *IAC* internal auditory canal, *IJV* internal jugular vein, *LSCD* lateral semicircular canal, *OC* otic capsule, *OCD* otic capsule dehiscence, *SSCD* superior semicircular canal dehiscence, *NDS* near dehiscence syndrome, *NIOCD* non-identified otic capsule dehiscence, *SPS* superior petrosal sinus, *PSC* posterior semicircular canal, *SSC* superior semicircular canal, *TW* third window

radiologists, and/or clinical audiologists to better understand some OCD variants and related TMWA, as well as to imagine possible innovative therapeutic approaches in the future. In some OCD variants, especially in those involving vascular structures (Type II OCD), MRI has greatly contributed to a better visualization of the anatomical elements in contact at the level of the TW, which has been an essential element for the current classification and for the development of new endovascular treatment techniques.

References

1. Merchant SN, Rosowski JJ. Conductive hearing loss caused by third-window lesions of the inner ear. Otol Neurotol. 2008;29(3):282–9. https://doi.org/10.1097/MAO.0b013e318161ab24.
2. Ho ML, Moonis G, Halpin CF, Curtin HD. Spectrum of third window abnormalities: semicircular canal dehiscence and beyond. AJNR Am J Neuroradiol. 2017;38(1):2–9. https://doi.org/10.3174/ajnr.A4922. PMID: 27561833; PMCID: PMC7963676.
3. Ho ML. Third window lesions. Neuroimaging Clin N Am. 2019;29(1):57–92. https://doi.org/10.1016/j.nic.2018.09.005.
4. Scarpa A, Ralli M, Cassandro C, Gioacchini FM, Greco A, Di Stadio A, Cavaliere M, Troisi D, de Vincentiis M, Cassandro E. Inner-ear disorders presenting with air-bone gaps: a review. J Int Adv Otol. 2020;16(1):111–6. https://doi.org/10.5152/iao.2020.7764. PMID: 32401207; PMCID: PMC7224429.
5. Ionescu E, Reynard P, Coudert A, Roiban L, Boudrigua AL, Thai-Van H. Superior semicircular canal dehiscence by superior petrosal sinus: proposal for classification. J Int Adv Otol. 2021;17(1):35–41. https://doi.org/10.5152/iao.2020.9384. PMID: 33605219; PMCID: PMC7901425.
6. Waldeck S, Lanfermann H, von Falck C, Froelich MF, Chapot R, Brockmann M, Overhoff D. New classification of superior semicircular canal dehiscence in HRCT. PLoS One. 2022;17(1):e0262758. https://doi.org/10.1371/journal.pone.0262758. PMID: 35051221; PMCID: PMC8775191.
7. Reynard P, Idriss S, Ltaief-Boudrigua A, Bertholon P, Pirvan A, Truy E, Thai-Van H, Ionescu EC. Proposal for a unitary anatomo-clinical and radiological classification of third mobile window abnormalities. Front Neurol. 2022;12:792545. https://doi.org/10.3389/fneur.2021.792545. PMID: 35087471; PMCID: PMC8786803.
8. Helmchen C, Gehrking E, Gottschalk S, et al. Persistence of perilymph fistula mechanism in a completely paretic posterior semicircular canal. J Neurol Neurosurg Psychiatry. 2005;76:280–2. https://doi.org/10.1136/jnnp.2004.038083.
9. Weinreich WM, Carey JP. Perilymphatic fistulas and superior semi-circular canal dehiscence syndrome. Adv Otorhinolaryngol. 2019;82:93–100. https://doi.org/10.1159/000490276.
10. Schuknecht HF. Otologic mystery. Am J Otol. 1987;8:182–3.
11. Iversen MM, Rabbitt RD. Wave mechanics of the vestibular semicircular canals. Biophys J. 2017;113:1133–49. https://doi.org/10.1016/j.bpj.2017.08.001.
12. Iversen MM, Rabbitt RD. Biomechanisms of third window syndrome. Front Neurol. 2020;11:891. https://doi.org/10.3389/fneur.2020.00891.
13. Grieser BJ, Kleiser L, Obrist D. Identifying mechanisms behind the tullio phenomenon: a computational study based on first principles. J Assoc Res Otolaryngol. 2016;17:103–18. https://doi.org/10.1007/s10162-016-0553-0.
14. Ward BK, Carey JP, Minor LB. Superior canal dehiscence syndrome: lessons from the first 20 years. Front Neurol. 2017;8:177. https://doi.org/10.3389/fneur.2017.00177.

15. Lund AD, Palacios SD. Carotid artery-cochlear dehiscence: a review. Laryngoscope. 2011;121(12):2658–60. https://doi.org/10.1002/lary.22391.
16. Wackym PA, Balaban CD, Zhang P, Siker DA, Hundal JS. Third window syndrome: surgical management of cochlea-facial nerve dehiscence. Front Neurol. 2019;10:1281. https://doi.org/10.3389/fneur.2019.01281.
17. Liu Z, Bi W, Li J, Li Q, Dong C, Zhao P, et al. Superior semicircular canal dehiscence in relation to the superior petrosal sinus: a potential cause of pulsatile tinnitus. Clin Radiol. 2015;70:943–7. https://doi.org/10.1016/j.crad.2015.04.017.
18. Wackym PA, Mackay-Promitas HT, Demirel S, Gianoli GJ, Gizzi MS, Carter DM, Siker DA. Comorbidities confounding the outcomes of surgery for third window syndrome: outlier analysis. Laryngosc Investig Otolaryngol. 2017;2(5):225–53. https://doi.org/10.1002/lio2.89. PMID: 29094067; PMCID: PMC5654938.
19. Ionescu EC, Al Tamami N, Neagu A, Ltaief-Boudrigua A, Gallego S, Hermann R, Truy E, Thai-Van H. Superior semicircular canal ampullae dehiscence as part of the spectrum of the third window abnormalities: a case study. Front Neurol. 2017;8:683. https://doi.org/10.3389/fneur.2017.00683. PMID: 29312118; PMCID: PMC5742101.
20. Matsuda H, Tanzawa Y, Sekine T, Matsumura T, Saito S, Shindo S, et al. Congenital Membranous stapes footplate producing episodic pressure-induced perilymphatic fistula symptoms. Front Neurol. 2020;11:585747. https://doi.org/10.3389/fneur.2020.585747.
21. Fröhlich L, Curthoys IS, Kösling S, Obrist D, Rahne T, Plontke SK. Cervical and ocular vestibular-evoked myogenic potentials in patients with intracochlear schwannomas. Front Neurol. 2020;11:549817. https://doi.org/10.3389/fneur.2020.549817.
22. Young YH, Wu CC, Wu CH. Augmentation of vestibular evoked myogenic potentials: an indication for distended saccular hydrops. Laryngoscope. 2002;112:509–12. https://doi.org/10.1097/00005537-200203000-00019.
23. Taylor RL, Zagami AS, Gibson WP, Black DA, Watson SR, Halmagyi MG, et al. Vestibular evoked myogenic potentials to sound and vibration: characteristics in vestibular migraine that enable separation from Menière's disease. Cephalalgia. 2012;32(3):213–25.
24. Wen MH, Cheng PW, Young YH. Augmentation of ocular vestibular-evoked myogenic potentials via bone-conducted vibration stimuli in ménière disease. Otolaryngol Neck Surg. 2012;146:797–803. https://doi.org/10.1177/0194599811433982.
25. Manzari L, Tedesco AR, Burgess AM, Curthoys IS. Ocular and cervical vestibular-evoked myogenic potentials to bone conducted vibration in Ménière's disease during quiescence vs during acute attacks. Clin Neurophysiol. 2010;121:1092–101. https://doi.org/10.1016/j.clinph.2010.02.003.
26. Muchnik C, Hildesheimer M, Rubinstein M, Arenberg IK. Low frequency air-bone gap in Menière's disease without middle ear pathology. A preliminary report. Am J Otol. 1989;10:1–4.
27. Yetişer S, Kertmen M. Cochlear conductive hearing loss in patients with Meniere's disease. Kulak Burun Bogaz Ihtis Derg. 2007;17:18–21.
28. Sugimoto S, Yoshida T, Teranishi M, Okazaki Y, Naganawa S, Sone M. The relationship between endolymphatic hydrops in the vestibule and low-frequency air-bone gaps. Laryngoscope. 2018;128:1658–62. https://doi.org/10.1002/lary.26898.
29. Wackym PA, Wood SJ, Siker DA, Carter DM. Otic capsule dehiscence syndrome: superior semicircular canal dehiscence syndrome with no radiographically visible dehiscence. Ear Nose Throat J. 2015;94:8–24. https://doi.org/10.1177/014556131509400802.
30. Wackym PA, Agrawal Y, Ikezono T, Balaban CD. Editorial: third window syndrome. Front Neurol. 2021;12:704095. https://doi.org/10.3389/fneur.2021.704095.
31. Curtin HD. Imaging of conductive hearing loss with a normal tympanic membrane. AJR Am J Roentgenol. 2016;206:49–56. https://doi.org/10.2214/AJR.15.15060.
32. Ward BK, Wenzel A, Ritzl EK, Gutierrez-Hernandez S, Della Santina CC, Minor LB, et al. Near-dehiscence: clinical findings in patients with thin bone over the superior semicircular canal. Otol Neurotol. 2013;34(8):1421–8. https://doi.org/10.1097/MAO.0b013e318287efe6.

33. Baxter M, McCorkle C, Trevino Guajardo C, Zuniga MG, Carter AM, Della Santina CC, Minor LB, Carey JP, Ward BK. Clinical and physiologic predictors and postoperative outcomes of near dehiscence syndrome. Otol Neurotol. 2019;40(2):204–12. https://doi.org/10.1097/MAO.0000000000002077. PMID: 30570606; PMCID: PMC6326856.
34. Mau C, Kamal N, Badeti S, Reddy R, Ying YM, Jyung RW, et al. Superior semicircular canal dehiscence: diagnosis and management. J Clin Neurosci. 2018;48:58–65. https://doi.org/10.1016/j.jocn.2017.11.019.
35. Creighton F Jr, Barber SR, Ward BK, Sharon JD, Carey JP. Underwater endoscopic repair of superior canal dehiscence. Otol Neurotol. 2020;41:560. https://doi.org/10.1097/MAO.0000000000002277.